doi.org/10.1002/hlca.202300131

RESEARCH ARTICLE

HELVETICA chimica acta

iso-Fatty Acid Metabolism in *Caenorhabditis elegans'* Ceramide Biosynthesis

Rocío Rivera Sánchez,[a] Siva Bandi,[a] Marie-Désirée Scheidt,[a] Hanna Laaroussi,[a] Bennett William Fox,[b] Yojiro Ishida,[c] Gaétan Glauser,[d] Sylvain Sutour,[d] and Stephan H. von Reuss*[a, d]

[a] Laboratory for Bioanalytical Chemistry, University of Neuchâtel, Avenue de Bellevaux 51, CH-2000 Neuchâtel, Switzerland, e-mail: stephan.vonreuss@unine.ch

[b] Boyce Thompson Institute and Department of Chemistry and Chemical Biology, Cornell University, 533 Tower Rd., Ithaca, NY 14853, USA

[c] Center for Advanced Biotechnology and Medicine (CABM), Rutgers University, 679 Hoes Ln W, Piscataway, NJ 08854, USA

[d] Neuchatel Platform for Analytical Chemistry (NPAC), University of Neuchâtel, Avenue de Bellevaux 51, CH-2000 Neuchâtel, Switzerland

Dedicated to Professor *Robert Deschenaux* on the occasion of his retirement

Ceramide biosynthesis and its connection to iso-fatty acid metabolism in the model organism *Caenorhabditis elegans* was investigated using a combination of reverse genetics and comparative ESI-(+)-HR-MS^e ceramide profiling along with incorporation experiments with bacterial mutants specifically enriched with isotopically labeled branched-chain amino acids or branched-chain fatty acids. Incorporation of a L-leucine-derived isovalerate unit into the conserved d17:1iso sphingosine building block proceeds through *elo-5* dependent chain elongation and depends on peroxisomal β-oxidation by the 3-ketoacyl-CoA thiolase *daf-22*, although ceramide profiles of N2 wildtype and *daf-22(ok693)* are indistinguishable. Biosynthesis of the homologous *N*-iso-acyl moieties also depends on L-leucine and isovalerate chain elongation but proceeds independently of *elo-5* and *daf-22*. Biosynthesis of the dominating *N*-docosanoyl moiety depends on *elo-3*-catalyzed chain elongation of bacteria-derived palmitic acid, whereas the *N*-tetracosanoyl moiety is derived from *de novo* lipogenesis.

Keywords: Biosynthesis, ceramide, *Caenorhabditis elegans*, iso-fatty acid, isotopic labeling, lipidomics, mass spectrometry, sphingolipids.

Introduction

Ceramides (*N*-acyl sphingosines, **6a**) represent the central hub in sphingolipid metabolism.[1] *De novo* ceramide biogenesis (*Scheme 1,a*) is initiated in the endoplasmic reticulum (ER) by condensation of a long chain acyl-CoA building block **1a** with L-serine (**2**). The resulting 3-keto-sphinganine **3a** is reduced to sphinganine (**4a**) and *N*-acylated to form dihydroceramides **5a**, that are finally dehydrogenated to ceramides **6a** by desaturase activity.[1–3] Ceramides **6a** constitute key building blocks for the assembly of complex sphingolipids such as sphingomyelins **7a** and glycosyl ceramides (**8a**, cerebrosides and gangliosides),[1–3] which have been implicated with a diversity of cellular functions including recognition, differentiation, senescence, and apoptosis[2–4] Conversely, sphingolipids (**7a** and **8a**) can be hydrolyzed in lysosomes as part of the 'salvage pathway' to recover ceramides **6a**,[5,6] which

Supporting information for this article is available on the WWW under https://doi.org/10.1002/hlca.202300131

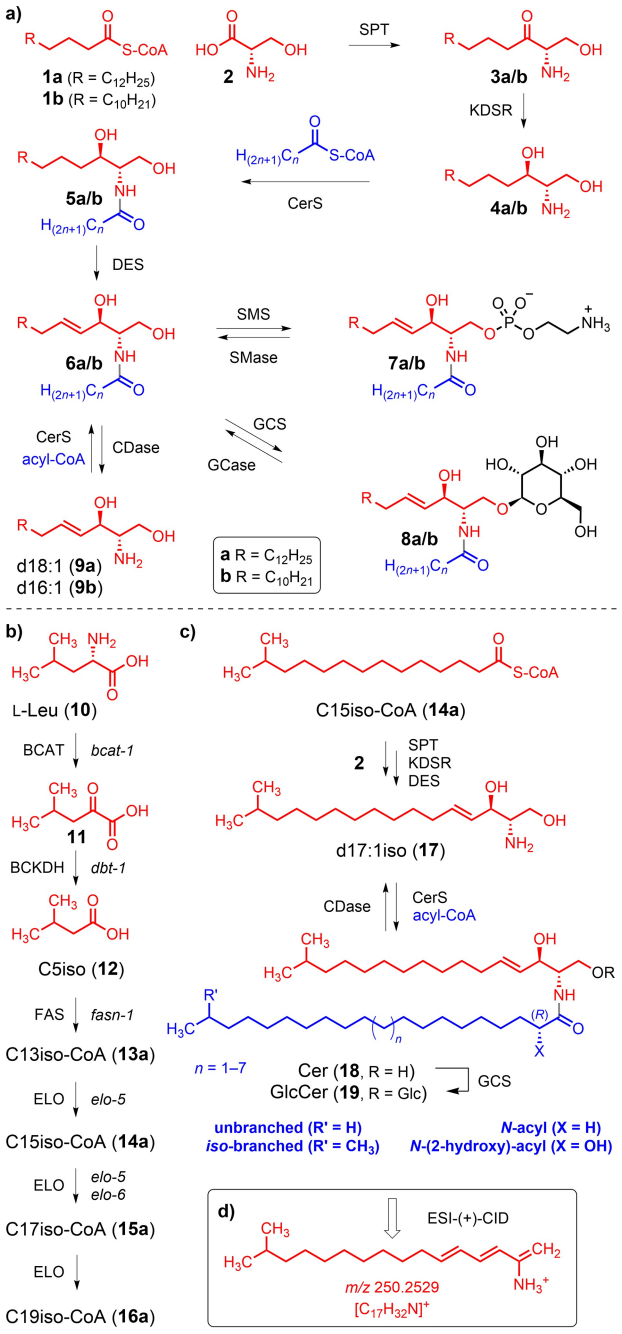

Scheme 1. a) Biosynthesis of unbranched ceramides and sphingolipids. b) *De novo* lipogenesis of branched chain iso-fatty acids (BCFA) in *C. elegans*. c) Biosynthesis of d17:1iso spingosine (**17**) based ceramides (**18**) and glycosylceramides (**19**) with *N*-acyl and *N*-iso-acyl side chains in *C. elegans*. d) ESI-(+)-HR-MS^e fragmentation utilized for ceramide profiling (SPT: serine palmitoyltransferase; KDSR: 3-keto-dihydrosphingosine reductase; CerS: ceramide synthase; DES: desaturase; SMS: sphingomyelin synthase; SMase: sphingomyelinase; GCS: glucosylceramide synthase; GCase: glucocerebrosidase; CDase: ceramidase; BCAT: branched chain amino acid transferase; BCKDH: branched chain α-ketoacid dehydrogenase; FAS: fatty acid synthase; ELO: elongase).

are ultimately metabolized and degraded through sphingosine (**9a**).[7,8]

Structural and functional ceramide diversity originates from attachment of homologous long chain *N*-acyl moieties by sidechain specific ceramide synthases (CerS),[9,10] whereas distinct sphingosine bases have been observed in animals, plants, and fungi.[11]

The bacterivorous nematode *Caenorhabditis elegans* represents a powerful model system to study lipid metabolism[12–14] and sphingolipid signaling,[15–18] which have been shown to involve *de novo* biosynthesis of iso-fatty acids (*Scheme 1,b*). *C. elegans'* cerebrosides (**19**, glucosyl-ceramides) have long been known to contain a specific iso-branched d17:1iso sphingosine unit (*4E*,15-methyl-d16:1)-sphingosine, **17**, that is *N*-acylated with saturated, straight and iso-branched-chain C20–C26 acids that can be 2-hydroxylated (*Scheme 1,c*).[19–21] Similar glycosyl ceramides were identified in the parasitic *Ascaris suum*.[22,23] Recent research has demonstrated that these glucosylceramides (GlcCer d17:1iso, **19**) promote postembryonic development,[24,25] foraging behavior,[26] lifespan,[27] and longevity,[28] and mediate survival of developmental arrest,[29] glucose response,[30] intestinal apical membrane polarity,[31] oocyte formation and early embryonic cell division[32] through «Target of Rapamycin Complex 1» (TORC1) signaling, which functions in nutrient sensing.[33]

Biosynthesis of the characteristic d17:1iso sphingosine building block **17** in *C. elegans* involves condensation of C15iso-CoA (**14a**) with L-serine (**2**; *Scheme 1,c*) and depends on two branched-chain fatty acids (BCFAs), C15iso (**14b**) and C17iso (**15b**) that are essential for *C. elegans* growth and development,[34–36] as well as ER homeostasis and lipid droplet growth.[37] Both BCFAs (**13**–**15**)[34] and d17:1iso sphingosine (**17**)[38] are derived from the branched chain amino acid (BCAA) L-leucine (**10**) through *de novo* lipogenesis[39] that is catalyzed by the fatty acid elongases *elo-5* and *elo-6*,[34] as well as the 3-ketoacyl-CoA reductase *let-767*[40] (*Scheme 1,b*). Mutation of *elo-5* results in developmental arrest at the first larval state (L1) that can be rescued by BCFA supplements.[34,35] Similarly, mutation of the branched chain α-ketoacid dehydrogenase (BCKDH) (*dbt-1*) causes BCFA deficiency and larval arrest, which can be rescued by BCFA supplements.[41,42] However, excess C17iso (**15b**) causes increased lethality under dietary restriction conditions mediated by glucosylceramides **19** through the TORC1 signaling pathway.[43]

Forward genetic screens in *elo-5* animals that can bypass developmental arrest from BCFA and glucosyl-

ceramide **19** deficiency have revealed several genes,[24,44] including *prx-5*[45] and *prx-11*[25] involved in peroxisome biogenesis and import. Silencing of the peroxisomal β-oxidation cycle involved in fatty acid metabolism and ascaroside biosynthesis,[46] by RNAi knock down of the 3-ketoacyl-CoA thiolase *daf-22* did not suppress the developmental L1 arrest phenotype of *elo-5(gk208)* and failed to rescue BCFA levels.[47] In contrast, knock down and knock-out of peroxisomal β-oxidation rescued the glucosylceramide **19** deficiency induced developmental arrest in glucosylceramide synthase (CGS) mutants, which are defective in glycosylation of ceramides (**18**; *Scheme 1,c*).[9,45] This intergenic suppression depends on the G-protein coupled receptor *daf-38* involved in ascaroside sensing,[48] indicating that β-oxidation dependent changes in ascaroside biosynthesis rescue the L1 arrest phenotype through hormonal ascaroside signaling downstream of the TORC1 pathway.[25]

Because C17iso fatty acid (**15b**) supplements are sufficient to rescue BCFA deficiency of *elo-5* loss of function mutants, which includes the C15iso-CoA building block (**14a**) required for d17:1iso sphingosine (**17**) biosynthesis, we aimed to decipher the potential importance of peroxisomal β-oxidation in iso-fatty acid metabolism and d17:1iso sphingosine biosynthesis upstream of ceramide biosynthesis. Using a combination of reverse genetics, comparative lipidomics, ceramide profiling by ESI-(+)-HR-MS^e, and isotope incorporation experiments with bacterial mutants specifically enriched with stable isotope labeled branched-chain amino acids (BCAA) and branched-chain fatty acids (BCFA) we characterize the biosynthetic connections between iso-fatty acid (**13**–**16**) metabolism and ceramide (**18**) biosynthesis. Our results demonstrate that ceramide (**18**) biosynthesis proceeds from L-leucine (**10**) through *elo-5* dependent *de novo* lipogenesis of C17iso-CoA (**15a**) and chain shortening to C15iso-CoA (**14a**) during the peroxisomal β-oxidation cycle catalyzed by the 3-ketoacyl-CoA thiolase *daf-22*, placing β-oxidation upstream of ceramide biosynthesis.

Results and Discussion

Ceramide (**18**) profiling of the *Caenorhabditis elegans* lipidome was performed by targeted HPLC-ESI-(+)-HR-MS analysis for previously described components (*Figure 1,a* and *1,b*)[16,19] all of which were also detected upon ESI-(+)-HR-MS^e screening (*Figure 1,c*) for the characteristic sphingosine-derived fragment ion at *m/z* 250.2529 $[C_{17}H_{32}N]^+$ as a highly sensitive marker signal (*Scheme 1,d*).[16,29,30,49] Isomeric structures were assigned based on the incorporation of branched-chain amino acids (BCAA). A total of 48 ceramides **18** were identified, which constitute a homologous series characterized by a conserved d17:1iso sphingosine (**17**) backbone that is *N*-acylated with straight and iso-branched acyl and 2-hydroxy-acyl moieties ranging from 16 to 27 carbons (*Figure 1,a*–*1,c*, *Tables S1* and *S2*). *C. elegans'* ceramides are dominated by Cer d17:1iso/22:0(2OH) (**18**, $n=3$, R′=H, X=OH) with a *N*-(2-hydroxy)docosanoyl moiety. The corresponding early eluting glucosylceramides **19** were also detected (*Table S3*). Targeted ESI-(+) and ESI-(−)-HR-MS analysis revealed only traces of dihydroceramides with a d17:0iso sphinganine (**34**) unit (*Scheme 2*) and no evidence for straight chain ceramides **6a**/**6b** based on

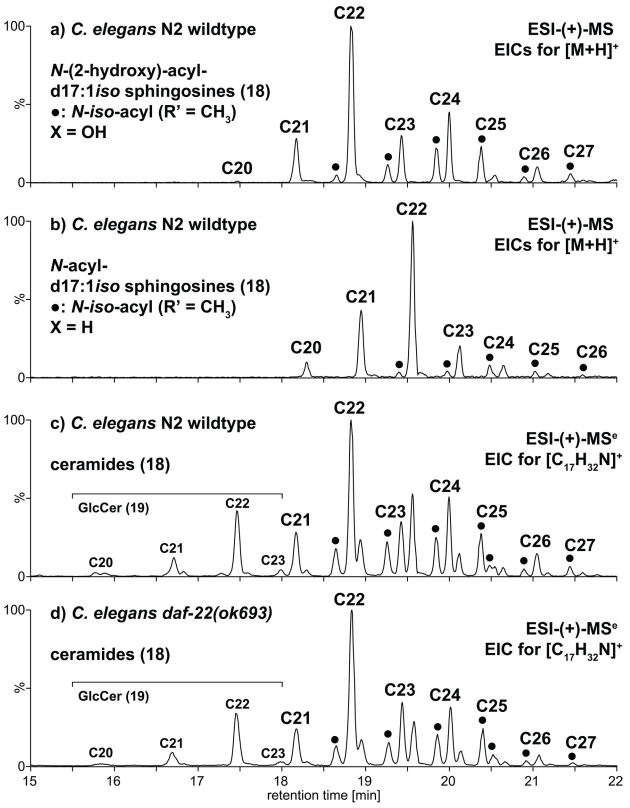

Figure 1. Targeted ceramide profiling of the *C. elegans* lipidome a) and b) by ESI-(+)-HR-MS extracted ion chromatograms for $[M+H]^+$ ions showing homologous series of isomeric *N*-(2-hydroxy)-acyl and *N*-acyl d17:1iso sphingosines (**18**), which could also be detected using *c*) ESI-(+)-HR-MS^e screening for the marker ion at *m/z* 250.2529 $[C_{17}H_{32}N]^+$. Comparative ESI-(+)-HR-MS^e ceramide profiling shows no significant difference between *c*) the *C. elegans* N2 wildtype and *d*) *daf-22(ok693)* mutant lipidome.

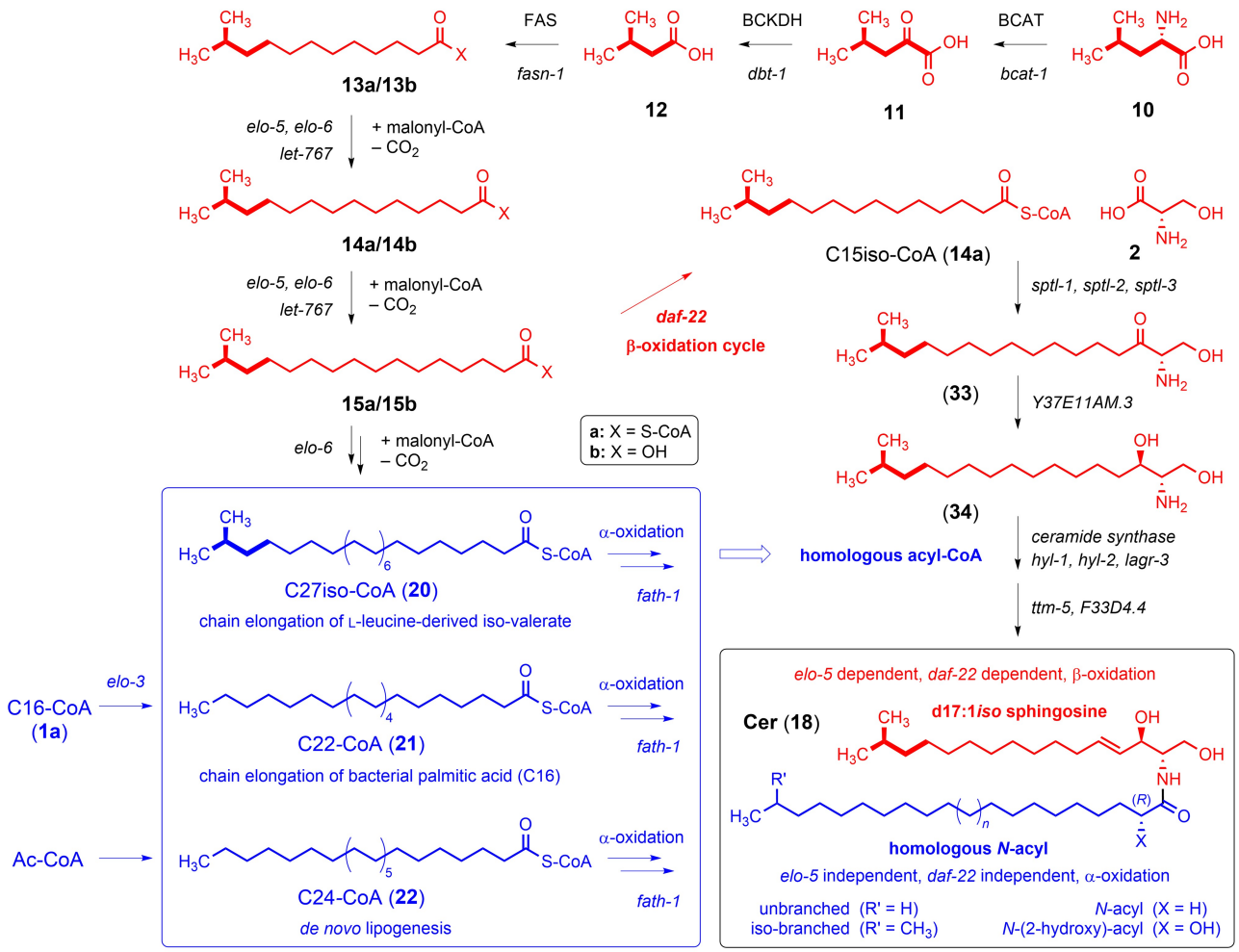

Scheme 2. Ceramide (**18**) biosynthesis in the model organism *C. elegans* includes the *de novo* biogenesis of the characteristic dC17:1iso sphingosine building block by *elo-5* dependent BCFA elongation of a L-leucine (**10**) derived isovalerate unit (**12**) to furnish C17iso-CoA (**15a**) as a substrate for the peroxisomal β-oxidation cycle to yield C15iso-CoA (**14a**) that condenses with L-serine (**2**) to give 3-ketosphinganine **33** and 17:0iso sphinganine **34**. In parallel, various lipogenic pathways give rise to very long chain fatty acid building blocks, such as the *elo-5* independent BCFA elongation of a L-leucine (**10**) derived isovalerate unit (**12**) to furnish C27iso-CoA (**20**), *elo-3* dependent chain elongation of bacteria-derived palmitoyl-CoA (**1a**) to furnish docosanoyl-CoA (**21**), or *de novo* lipogenesis to yield tetracosanoyl-CoA (**22**). These fatty acid building blocks are processed by the α-oxidation cycle and *fath-1* dependent 2-hydroxylation to furnish a homologous series of *N*-acyl and *N*-(2-hydroxy)-acyl building blocks that are attached to the d17:1iso sphingosine backbone (**17**) by ceramide synthases to generate a modular library of ceramides (**18**) as building blocks for complex sphingolipids.

the d18:1 sphingosine (**9a**) or d16:1 sphingosine (**9b**) backbone (*Scheme 1,a*).

C. elegans' ceramides **18** are enriched in the lipidome but are also released into the environment (*Figure S1*). Comparative ESI-(+)-HR-MS^e analysis of diverse nematodes demonstrated that ceramide profiles are highly conserved among different *C. elegans* strains, including the common laboratory strain N2 (Bristol) and two wild isolates from Australia and Hawaii, and more broadly within the *Caenorhabditis* genus (Rhabditidae), such as its recently identified sister species *C. inopinata*,[50] and the closely related *C. briggsae*, *C. brenneri*, *C. nigoni*, *C. remanei*, *C. tropicalis*, and *C. wallacei* (*Figure S2*).[51] The same ceramides were also detected in more distantly related species such as *Pristionchus pacificus* (Diplogasteridae), *Panagrellus redivivius* and *Turbatrix aceti* (Panagrolaimidae), as well as the entomopathogenic *Heterorhabditis bacteriophora* (Heterorhabditidae) and *Steinernema carpocapsae* (Steinernematidae; *Figure S2*). No ceramides based on d18:1 sphingosine (**9a**) or d16:1

sphingosine (**9b**) could be observed in any of these species.

In order to elucidate the potential function of the peroxisomal β-oxidation cycle in ceramide biosynthesis, comparative ESI-(+)-HR-MS^e ceramide profiling of the *C. elegans* wildtype and *daf-22(ok693)* lipidome was performed, which did not reveal any significant differences (*Figure 1c*, and *1,d*). Similarly, screening diverse peroxisomal trafficking mutants (*prx*), that have been reported to suppress the glucosylceramide **19**-mediated developmental L1 arrest,[25,45] such as *prx-1(tm392)*, *prx-3(tm6469)*, *prx-5(ku517)*, *prx-5(tm4948)*, and *prx-10(ssd68)* did not reveal any changes in ceramide **18** profiles (*Figure S3*) in agreement with the conclusion that they act downstream of glucosylceramide **19** biosynthesis.[25]

Considering that ceramides **18** based on the characteristic branched chain d17:1iso sphingosine (**17**) unit are widely conserved in nematodes, we aimed to decipher their biosynthetic origin by incorporation experiments with stable isotope labeled branched-chain amino acids (BCAAs) and branched-chain fatty acids (BCFAs). Because free amino acid supplements of monoxenic *C. elegans* cultures fed with metabolically active bacteria can lead to limited incorporation, extensive isotope dilution and scrambling, we took advantage of the tractable genetics of *E. coli*, which is the standard diet for bacterivorous *C. elegans*.

Feeding *C. elegans* with an auxotrophic *E. coli* BL21(DE3) *ΔilvD ΔleuB ΔavtA ΔilvE* mutant, defective in BCAA biosynthesis and metabolism and specifically enriched with 50% L-[U-$^{13}C_6$]-leucine ([$^{13}C_6$]-**10**) furnished ceramides with an [$^{13}C_5$]–d17:1iso sphingosine base ([$^{13}C_5$]-**17**) as shown by ESI-(+)-HR-MS^e fragments at *m/z* 255.2697 [$^{12}C_{12}{}^{13}C_5H_{32}N]^+$ (*Figure 2,a*). In contrast, feeding L-[U-$^{13}C_5$]-valine enriched *E. coli* did not result in [^{13}C]-labeled ceramides. Interestingly, we found that the incorporation of L-[U-$^{13}C_6$]-leucine ([$^{13}C_6$]-**10**) into [$^{13}C_5$]-ceramides ([$^{13}C_5$]-**18**) depends on the peroxisomal β-oxidation cycle. [$^{13}C_5$]-Enrichment of the d17:1iso sphingosine moiety ([$^{13}C_5$]-**17**) from isotopic labeling is strongly reduced (to approximately 10% of wildtype) in the peroxisomal 3-ketoacyl-CoA thiolase mutant *daf-22(ok693)* (*Figure 2,b*), suggesting that the C15iso-CoA building block (**14a**) that reacts with L-serine (**2**) to form the d17:1iso sphingosine (**17**) unit (*Scheme 1,c*) is derived from chain shortening of C17iso-CoA (**15a**) through DAF-22-dependent β-oxidation and not directly through *de novo* synthesized C15iso-CoA (**14a**). While *daf-22* is essential for the incorporation of L-[U-$^{13}C_6$]-leucine ([$^{13}C_6$]-**10**) into

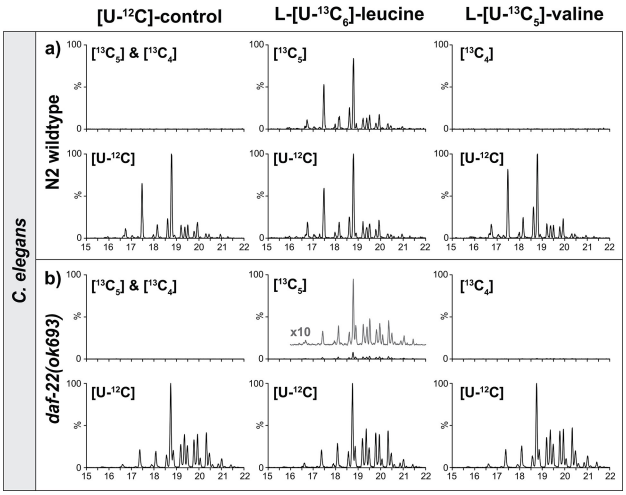

Figure 2. ESI-(+)-HR-MS^e ceramide (**18**) profiling using marker ions at *m/z* 250.2529 $[C_{17}H_{32}N]^+$, *m/z* 254.2663 [$^{12}C_{13}{}^{13}C_4H_{32}N]^+$ and *m/z* 255.2697 [$^{12}C_{12}{}^{13}C_5H_{32}N]^+$ shows incorporation of L-[U-$^{13}C_6$]-leucine (**10**, 50% enrichment) into the [$^{13}C_5$]–d17:1iso sphingosine building block (**17**) in *C. elegans* wildtype, which is strongly suppressed in the *daf-22(ok693)* mutant.

[$^{13}C_5$]–d17:1iso sphingosine ([$^{13}C_5$]-**17**) in *C. elegans*, comparative ceramide profiling of the N2 wildtype and *daf-22(ok693)* mutant lipidomes revealed only very minor differences (*Figure 1,c* and *1,d*), demonstrating that *de novo* biogenesis of d17:1iso sphingosine (**17**) is compensated by a yet unidentified mechanism.

Careful analysis of the ESI-(−)-HR-MS molecular ion signals revealed the incorporation of one L-[U-$^{13}C_6$]-leucine (**10**) derived [$^{13}C_5$]-isovalerate unit (**12**) for ceramide isomers with straight *N*-acyl chains (*Figure 3,b*), whereas those with *N*-iso-acyl residues show a distribution of [^{13}C]-isotopomers corresponding to the incorporation of up to two [$^{13}C_5$]-units, in agreement with an L-[U-$^{13}C_6$]-leucine origin for both the d17:1iso sphingosine and the *N*-iso-acyl building blocks.

While the [$^{13}C_5$]-enrichment of the d17:1iso sphingosine unit (**17**) upon feeding with L-[U-$^{13}C_6$]-leucine ([$^{13}C_6$]-**10**) enriched *E. coli* is largely suppressed in the *daf-22(ok693)* mutant, the ceramide isomers carrying branched-chain *N*-iso-acyl units are still efficiently [$^{13}C_5$]-labeled (*Figure 3,c*) demonstrating that the biosynthesis of the homologous series of *N*-iso-acyl building blocks (*Scheme 1,b*) is independent of the β-oxidation cycle. Inspection of ESI-(−)-HR-MS^e spectra also confirmed that the [$^{13}C_5$]-labels are exclusively located in the homologous *N*-iso-acyl building blocks. Taken together, these results demonstrate that the biogenesis of *N*-iso-acyl substituted ceramides **18** (R′ = CH_3) in wildtype *C. elegans* incorporates two L-leucine

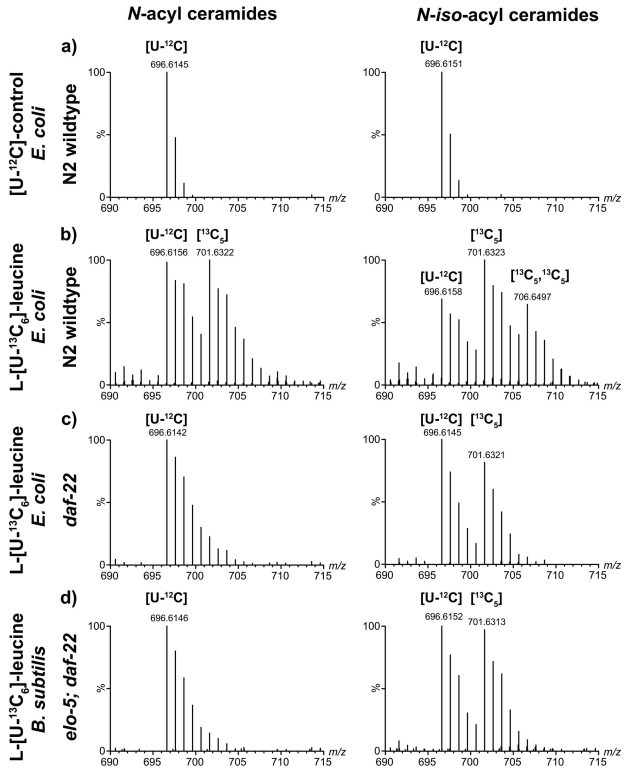

Figure 3. Representative ESI-(−)-HR-MS spectra of the $[M+HCOO]^-$ molecular ion adducts for ceramides (**18**) carrying *N*-tetracosanoyl or *N*-iso-tetracosanoyl moieties from a) natural abundance (control) experiments, b) L-[U-$^{13}C_6$]-leucine enriched *E. coli* BL21(DE3) *ΔilvD ΔleuB ΔavtA ΔilvE* mutant fed to *C. elegans* N2 wildtype or c) the *daf-22(ok693)* mutant, or d) L-[U-$^{13}C_6$]-leucine and [$^{13}C_5$]-BCFA enriched *B. subtilis ilvB2 leuA169* fed to *C. elegans elo-5(gk208); daf-22(ok693)* double mutant.

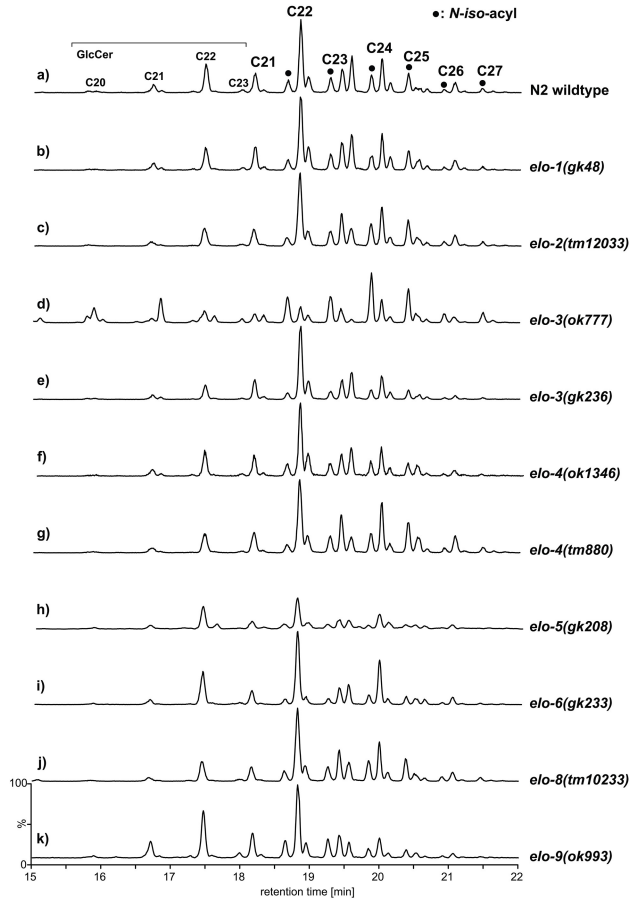

Figure 4. ESI-(+)-HR-MS^e ceramide (**18**) profiles in *C. elegans* N2 wildtype and fatty acid elongase (*elo*) mutants using the marker ion at *m/z* 250.2529 $[C_{17}H_{32}N]^+$.

(**10**) derived isovalerate (**12**) units in the d17:1iso sphingosine (**17**) and *N*-iso-acyl moieties, respectively, and further indicates that these two iso-acyl building blocks are derived from two distinct biosynthetic pathways, the *daf-22* dependent *de novo* biogenesis of d17:1iso sphingosine (**17**) and the *daf-22* independent lipogenesis of very long chain iso-fatty acids (*Scheme 2*).

The incorporation of a leucine (**10**) derived isovalerate (**12**) unit into odd numbered iso-fatty acids **13b**–**16b** requires consecutive chain elongation steps catalyzed by specific fatty acid elongases (*elo*; *Figure 1,b*).[52] Comparative analysis of ceramide profiles in a variety of *elo*-mutants confirmed that ceramide **18** abundance is most dramatically reduced in the *elo-5(gk-208)* mutant (*Figure 4*) that is defective in BCFA elongation.[34,35] Supplementation with synthetic C17iso (**15b**) rescues the developmental arrest, but the *elo-5(gk-208)* ceramide profile contains only limited amounts of *N*-acyl d17:1iso sphingosines **18**, and is instead dominated by homologous ceramides **6b** with an unbranched d16:1 sphingosine building block (**9b**; *Figure S4,a*).[40] The *elo-6(gk233)* lipidome showed reduced quantities of ceramides with *N*-iso-acyl moieties, suggesting the involvement of *elo-6* in chain elongation of very long chain iso-fatty acids such as C27iso-CoA (**20**; *Scheme 2*). Furthermore, relative abundance of *N*-(2-hydroxy)-docosanoyl d17:1iso sphingosine (Cer d17:1iso/22:0(2OH), **18**, $n=3$, X=OH, R′=H), the dominating ceramide observed in diverse nematodes (*Figure S2*), is strongly attenuated in *elo-3(ok777)* (but not in *elo-3(gk236)*; *Figure 4*), in agreement with *elo-3* dependent biosynthesis of docosanoyl-CoA (**21**) as a precursor for GlcCer d17:1iso/22:0 **19** ($n=3$, X=H, R′=H) involved in *C. elegans* longevity.[28]

Mixed isotope labeling by feeding *C. elegans* with a 1:1 mixture of [U-^{12}C]- and [U-^{13}C]-*E. coli*[37] furnished Cer d17:1iso/22:0(2OH) **18** ($n=3$, X=OH, R′=H) with a

bimodal distribution of ^{13}C isotopomers (*Figure 5*) that confirms the biogenetic origin of the docosanoyl-CoA building block (**21**) from *elo-3*-catalyzed chain elongation of bacteria-derived palmitoyl-CoA (**1a**), whereas the tetracosanoyl-CoA precursor (**22**) for Cer d17:1iso/24:0(2OH) **18** ($n=5$, X=OH, R′=H), which is not suppressed in *elo-3(ok777)*, originates from *de novo* lipogenesis, demonstrating that ceramide *N*-acyl residues in *C. elegans* are derived from diverse biosynthetic pathways (*Scheme 2*).

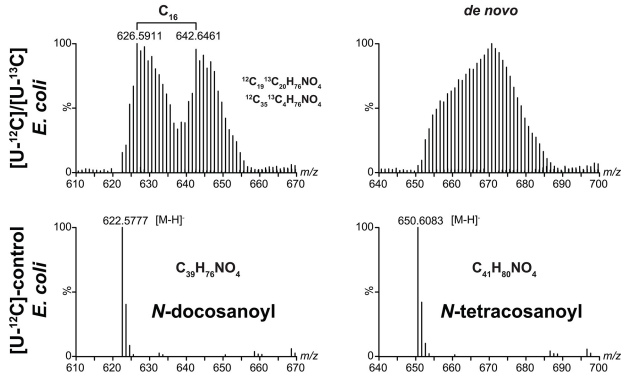

Figure 5. ESI-(−)-HR-MS spectra of ceramides (**18**) show distinct distributions of ^{13}C isotopomers upon mixed isotope labeling by feeding a 1:1 mixture of [U-^{12}C] and [U-^{13}C]-*E. coli*, indicating chain elongation of bacteria-derived palmitoyl-CoA (**1a**, C16) for the *N*-docosanoyl moiety (**21**) of Cer d17:1iso/22:0(2OH) and *de novo* lipogenesis for the *N*-tetracosanoyl moiety (**22**) of Cer d17:1iso/24:0(2OH).

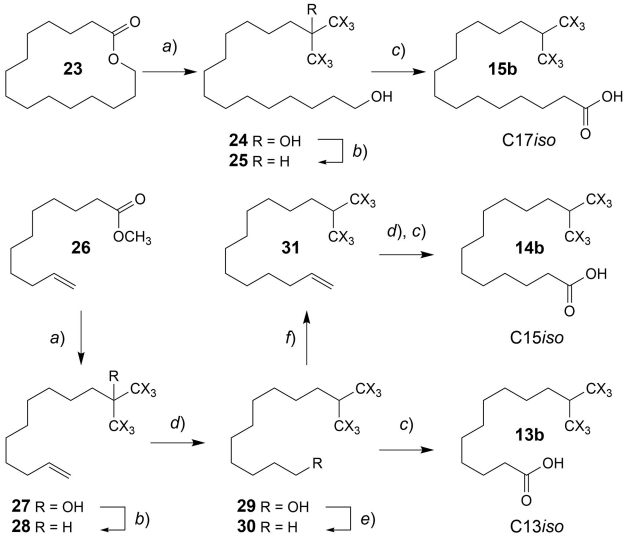

Scheme 3. Synthesis of iso-fatty acids C13iso (**13b**), C15iso (**14b**), and C17iso (**15b**) and their [D_6]-isotopomers (X=D). Reagents: a) CH_3MgI or CD_3MgI; b) BF_3, Et_3SiH; c) $KMnO_4$; d) 1. BH_3, 2. H_2O_2; e) PPh_3, Br_2; f) vinyl magnesium bromide, $Li_2[CuCl_4]$.

In order to unambiguously establish the importance of BCFA metabolism in *C. elegans* d17:1iso sphingosine and *N*-iso-acyl ceramide biosynthesis, iso-fatty acids C13iso (**13b**), C15iso (**14b**), and C17iso (**15b**) were synthesized as shown in *Scheme 3*. C17iso (**15b**) was available in three steps from pentadecanolide (**23**) by addition of methyl magnesium iodide and selective deoxygenation of the resulting tertiary alcohol **24** with boron trifluoride and triethylsilane, followed by permanganate oxidation of the primary alcohol **25** as previously described.[53] Similarly, C13iso (**13b**) and C15iso (**14b**) were accessible from methyl 10-undecenoate (**26**) by reaction with methyl magnesium iodide and deoxygenation followed by *anti*-Markovnikov hydration of **28** or **31** to furnish the primary alcohols **29** and **32** that were converted to C13iso (**13b**) and C15iso (**14b**) by permanganate oxidation, respectively.[53] Homologation of iso-tridecene **28** to iso-pentadecene **31** was accomplished by cuprate(II) catalyzed coupling of the iso-tridecyl bromide **30** with vinyl magnesium bromide. The corresponding stable isotope labeled [D_6]-iso-fatty acids (X=D) were prepared by substituting natural abundance with [D_3]-labeled methyl magnesium iodide. The homologous iso-fatty acids **13b**–**15b** and their [D_6]-isotopomers were subsequently employed as molecular probes to study BCFA metabolism and ceramide biogenesis in *C. elegans*.

Rearing the axenized *elo-5(gk208)* loss of function mutant on a nonpermissive *E. coli* diet (devoid of BCFAs) resulted in developmental arrest, which could be rescued by supplementation with free iso-fatty acids (**13b**, **14b**, or **15b**) but ceramide levels could not be fully recovered. Incorporation of [D_6]-labeled iso-fatty acids [D_6]–C13iso ([D_6]-**13b**), [D_6]–C15iso ([D_6]-**14b**), and [D_6]–C17iso ([D_6]-**15b**) furnished highly enriched ceramides **18** carrying [D_6]–d17:1iso sphingosine building blocks **17** with up to 90% [D_6]-enrichment as shown by the relative intensity of the ESI-(+)-HR-HR-MS^e fragment ion at *m/z* 256.2906 $[C_{17}H_{26}D_6N]^+$ (*Figure 6,a*). Comparable to the incorporation of L-[U-$^{13}C_6$]-leucine ([$^{13}C_6$]-**10**) into [$^{13}C_5$]-sphingosine ([$^{13}C_5$]-**17**), the incorporation of [D_6]-iso-fatty acids ([D_6]-**13b**, [D_6]-**14b**, [D_6]-**15b**) into [D_6]-sphingosine ([D_6]-**17**) depends on the peroxisomal β-oxidation cycle and is strongly attenuated (but not completely abolished) in the *elo-5(gk208); daf-22(ok693)* double mutant (*Figure 6,b*).

Only [D_6]-mono-labeled ceramides [D_6]-**18** were observed upon incorporation of [D_6]-BCFAs in *elo-*

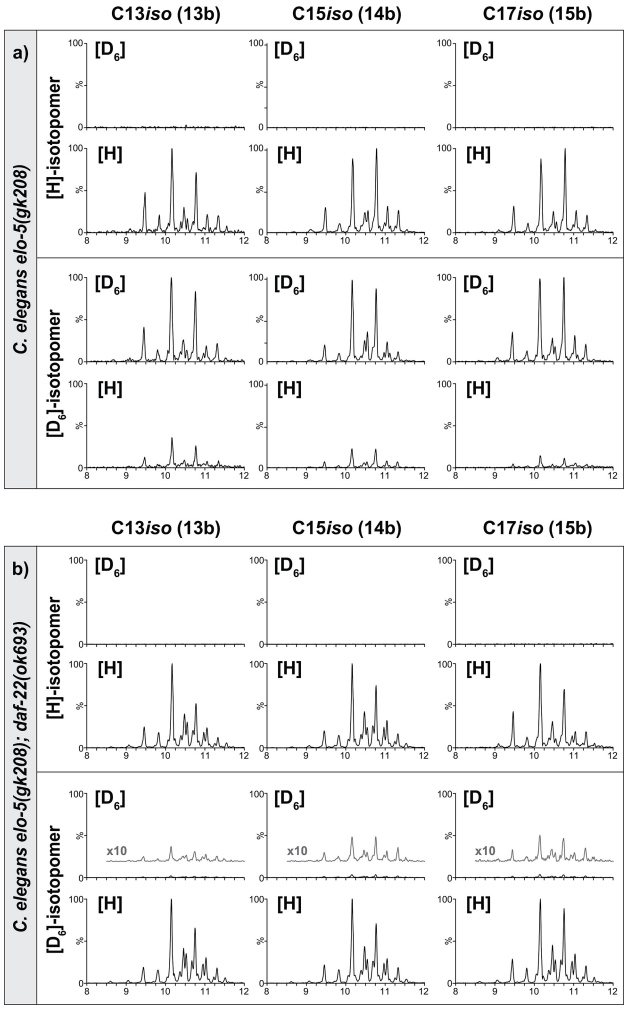

Figure 6. ESI-(+)-HR-MS^e ceramide profiling using the marker ions at *m/z* 250.2529 $[C_{17}H_{32}N]^+$ and *m/z* 256.2906 $[C_{17}H_{26}D_6N]^+$ shows incorporation of $[D_6]$-iso-fatty acids (**13b**–**15b**, >99% enrichment) into the $[D_6]$–d17:1iso sphingosine (**17**) building block of ceramides (**18**) in *C. elegans elo-5(gk208)*, which is strongly suppressed in the *elo-5(gk208); daf-22(ok693)* double mutant.

5(gk208) (*Figure S5*) and the $[D_6]$-label was exclusively located in the d17:1iso sphingosine moiety (**17**). No significant $[D_6]$-enrichment of the very long chain *N*-iso-acyl building blocks could be detected, demonstrating that the *daf-22*-independent pathway from L-leucine (**10**) to very long chain iso-fatty acids such as C27iso-CoA (**20**; *Scheme 2*) does not efficiently incorporate exogenous BCFAs, suggesting that it is independent of the fatty acid elongase *elo-5*.

Targeted ESI-(−)-analysis for free odd numbered iso-fatty acids in the *C. elegans* lipidome revealed an alternating series from C15iso (**14b**) till C27iso (**20**; *Figure S6*) that is strongly dominated by C15iso (**14b**) and C17iso (**15b**), all of which were $[^{13}C_5]$-labeled upon incorporation of L-[U-$^{13}C_6$]-leucine (**10**) in N2 wildtype and *daf-22(ok693)*. In contrast, free BCFA profiles in *elo-5(gk208)* depend on the iso-fatty acid supplement utilized to rescue the developmental arrest phenotype (*Figure 7,a–7,c*). Contradicting the general assumption that *elo-5* is essential for elongation of C13iso-CoA (**13a**) to C15iso-CoA (**14a**),[34,35] analysis of the *elo-5(gk208)* loss of function mutant supplemented exclusively with C13iso (**13b**) revealed free C15iso (**14b**), C17iso (**15b**), and C19iso (**16b**), demonstrating *elo-5* independent elongation of C13iso (**13b**; presumably by *elo-6*; *Figure 7,a*), which was unambiguously established by elongation of

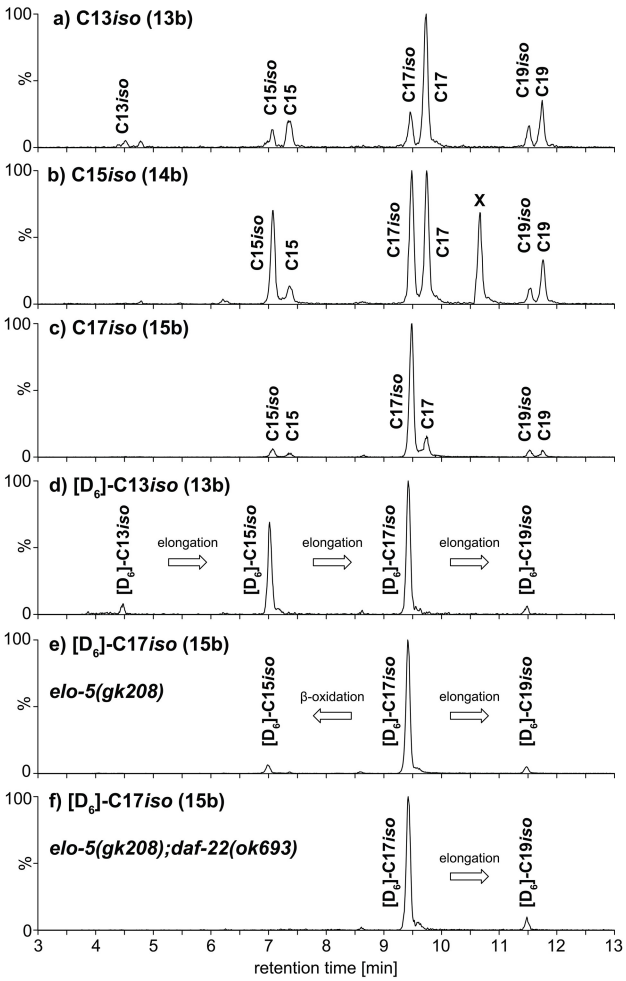

Figure 7. Targeted ESI-(−)-HR-MS profiling of free BCFAs using EICs for $[M-H]^-$ in *a*)–*e*) *elo-5(gk208)* or *f*) in *elo-5(gk208); daf-22(ok693)* supplemented with *a*) C13iso (**13b**), *b*) C15iso (**14b**), *c*) C17iso (**15b**), *d*) $[D_6]$–C13iso (D_6)-**13b**), or *e*) and *f*) $[D_6]$–C17iso (D_6)-**15b**), shows *elo-5*-independent elongation of C13iso (**13b**; *a*) and *d*)) and *daf-22*-dependent chain shortening of C17iso (**15b**; *e*) and *f*)).

[D_6]–C13iso ([D_6]-**13b**; *Figure 7,d*). Likewise, exogenous C15iso (**14b**) and C17iso (**15b**) were effectively elongated into C17iso (**15b**) and C19iso (**16b**), respectively (*Figure 7b* & c). Interestingly, C17iso (**15b**) was also shortened to C15iso (**14b**), which was unambiguously established by application of [D_6]–C17iso ([D_6]-**15b**; *Figure 7,e*). Chain shortening of [D_6]–C17iso ([D_6]-**15b**) depends on the peroxisomal β-oxidation cycle and is suppressed in the *elo-5(gk208); daf-22(ok693)* double mutant (*Figure 7,f*), providing a molecular basis for the deficiency of the *daf-22(ok693)* mutant to incorporate isotopically labeled L-leucine (**10**; *Figure 2*) and BCFAs **13b**–**15b** (*Figure 6*) into d17:1iso sphingosine (**17**), which implies that the C15iso-CoA building block (**14a**) that condenses with L-serine (**2**) is derived from peroxisomal β-oxidation of C17iso-CoA (**15a**) and not directly through *de novo* lipogenesis of C15iso-CoA (**14a**; *Scheme 2*).

Aiming to compensate for the limited solubility and uptake of exogenous free iso-fatty acid supplements by the *elo-5(gk208)* mutant, *Bacillus subtilis* was employed as an alternative bacterial food source rich in BCFAs, especially C15iso (**14b**) and C17iso (**15b**), along with C15*anteiso* and C17*anteiso*.[54] Feeding *elo-5(gk208)* with *Bacillus subtilis* effectively rescues the developmental L1 arrest phenotype and fully recovers ceramide profiles with the nematode specific d17:1iso sphingosine building block (**17**), while resulting in the disappearance of d16:1-sphingosine (**9b**) based ceramides (**6b**) that are observed with the free BCFA supplements (*Figures S4,a* and *S4,b*). Feeding the *elo-5(gk208); daf-22(ok693)* double mutant with an auxotrophic *Bacillus subtilis ilvB2 leuA169* mutant defective in BCAA biosynthesis that has been selectively enriched with 50% L-[U-$^{13}C_6$]-leucine ([$^{13}C_6$]-**10**) to function as a rich source of L-[U-$^{13}C_6$]-leucine labeled proteins and [$^{13}C_5$]–C15iso ([$^{13}C_5$]-**14b**) and [$^{13}C_5$]–C17iso ([$^{13}C_5$]-**15b**) labeled lipids furnished [$^{13}C_5$]-ceramides [$^{13}C_5$]-**18** (*Figure 3,d*) with homologous [$^{13}C_5$]-*N*-iso-acyl building blocks (*Figure S4,c*), but devoid of any [$^{13}C_5$]-enrichment for the conserved d17:1iso sphingosine backbone (**17**; *Figure S4,d*), which confirms that *de novo* biogenesis of d17:1iso sphingosine (**17**) through the incorporation of L-leucine (**10**) derived C15iso-CoA (**14a**) depends on peroxisomal β-oxidation by the 3-ketoacyl-CoA thiolase *daf-22*.

Targeted ESI-(+)-HR-MS screening of the *C. elegans* lipidome for 3-ketosphinganine **33** and sphinganine **34**, the biosynthetic intermediates in d17:1iso sphingosine (**17**) biosynthesis (*Scheme 2*), revealed only limited quantities, which are effectively [$^{13}C_5$]-labeled upon incorporation of L-[U-$^{13}C_6$]-leucine (**10**) as previously reported (*Figure S7*).[38] In contrast to the downstream ceramides (*N*-acyl d17:1iso sphingosines **18**), 3-ketosphinganine **33** and sphinganine **34** are partially [$^{13}C_5$]-labeled upon incorporation of L-[U-$^{13}C_6$]-leucine (**10**) enriched *E. coli ΔilvD ΔleuB ΔavtA ΔilvE* in the *daf-22(ok693)* mutant (*Figure S7*), which confirms that *de novo* d17:1iso sphingosine (**17**) biosynthesis is not completely abolished in *daf-22(ok693)*, and which also suggests that the unlabeled d17:1iso sphingosine (**17**) building block in ceramides **18** of *daf-22(ok693)* does not originate from a L-leucine (**10**) and *daf-22* independent pathway, but is most likely derived from sphingolipid recycling.

Conclusions

C. elegans' ceramides **18** represent a highly conserved class of nematode-derived modular metabolites (NDMMs) that integrate building blocks from diverse biosynthetic pathways. Structural and functional diversity of ceramides originates from the homologous series of *N*-acyl building blocks that are attached by sidechain specific ceramide transferases[10,15] and which originate from different lipogenic pathways. *N*-iso-acyl moieties ranging from C17iso to C27iso originate from a L-leucine (**10**) derived isovalerate unit (**12**) through chain elongation of BCFAs until the very long chain C27iso-CoA (**20**; *Table 1*, *Scheme 2*). The absence of incorporation of isotopically labeled BCFAs into *N*-iso-acyl building blocks in *elo-5(gk208)* loss of function mutants (*Table 1*) suggests that this pathway is independent of *elo-5* and apparently operates in parallel to the *elo-5* dependent chain elongation of BCFAs implicated in *de novo* d17:1iso sphingosine (**17**) biogenesis. Downregulation of iso-branched ceramides in the *elo-6(gk233)* ceramide profile (*Figure 4*) might suggest the involvement of *elo-6*. The *N*-docosanoyl moiety represents the most abundant building block observed in *C. elegans* ceramides, both with respect to *N*-acyl and *N*-(2-hydroxy)acyl residues. Their abundance is strongly attenuated in the *elo-3(ok777)* mutant and depends on chain elongation of bacteria-derived palmitoyl-CoA (**1a**) to docosanoyl-CoA (**21**) as previously described (*Scheme 2*).[28] In contrast, ceramides with the homologous *N*-tetracosanoyl moiety are independent of *elo-3* and originate from *de novo* lipogenesis of tetracosanoyl-CoA (**22**). *C. elegans'* ceramides consequently integrate diverse lipogenic pathways by attachment of homologous long chain *N*-acyl and *N*-iso-acyl moieties catalyzed by

Table 1. Summary of the stable isotope labeling incorporation experiments.

C. elegans	wildtype[a,b] *elo-5(gk208)*[c,d]		*daf-22(ok693)*[a–d]	
	d17:1iso-(**17**)	*N*-iso-acyl	d17:1iso-(**17**)	*N*-iso-acyl
L-[U-$^{13}C_6$]-leucine[a]	[$^{13}C_5$]	[$^{13}C_5$]	–	[$^{13}C_5$]
L-[U-$^{13}C_5$]-valine[b]	–	–	–	–
[D_6]-BCFA[c]	[D_6]	–	–	–
[^{13}C]-*B. subtilis*[d]	[$^{13}C_5$]	[$^{13}C_5$]	–	[$^{13}C_5$]

[a] L-[U-$^{13}C_6$]-leucine (**10**) enriched *E. coli* BL21(DE3) *ΔilvD ΔleuB ΔavtA ΔilvE.* [b] L-[U-$^{13}C_5$]-valine enriched *E. coli* BL21(DE3) *ΔilvD ΔleuB ΔavtA ΔilvE.* [c] C13iso (**13b**), [D_6]–C15iso (**14b**), or [D_6]–C17iso (**15b**) supplemented *E. coli.* [d] L-[U-$^{13}C_6$]-leucine (**10**) and [$^{13}C_5$]-BCFA **13b**–**15b** enriched *B. subtilis ilvB2 leuA169.*

sidechain specific (dihydro)ceramide synthases.[15,55–57] The occurrence of continuous homologous series of *N*-acyl and *N*-iso-acyl ceramides (distinct from the alternating series of fatty acids derived from chain elongation and chain shortening upon lipogenesis and peroxisomal β-oxidation, resp.) suggests that the different lipogenic inputs are processed through the peroxisomal α-oxidation cycle prior to their attachment to the d17:1iso-sphingosine (**17**) backbone (*Scheme 2*). Finally, the various *N*-acyl building blocks are partially hydroxylated at the 2-position by fatty acid 2-hydroxylase (*fath-1*).[43,58]

The biosynthesis of the characteristic d17:1iso sphingosine unit (**17**), the conserved key building block of ceramides in all nematode species analyzed so far, depends on a L-leucine (**10**) derived isovalerate (**12**) unit and proceeds through *elo-5* dependent chain elongation of BCFAs (*Scheme 2*). In the *elo-5(gk208)* mutant defective in BCFA biosynthesis, supplements of C13iso (**13b**), C15iso (**14b**), or C17iso (**15b**) are required to rescue the developmental L1 arrest phenotype and these exogenous BCFAs are efficiently incorporated into the d17:1iso sphingosine unit (**17**; *Table 1*). However, the incorporation of L-leucine (**10**) and the BCFAs **13b**–**15b** into d17:1iso sphingosine (**17**) depends on the peroxisomal β-oxidation cycle and is strongly attenuated (but not fully abolished) in the 3-ketoacyl-CoA thiolase mutant *daf-22(ok693)* and the *elo-5(gk208); daf-22(ok693)* double mutant, respectively (*Table 1*). While free BCFA supplements rescue developmental arrest of *elo-5(gk208)* and *elo-5(gk208); daf-22(ok693)* mutants, they do not fully recover ceramide profiles but instead result in the formation of an unusual series of ceramides **6b** that carry a straight chain d16:1 sphingosine (**9b**) building block (*Scheme 1*). Utilizing the BCAA auxotrophic *Bacillus subtilis ilvB2 leuA169* mutant as a rich source of L-[U-$^{13}C_6$]-leucine (**10**) enriched proteins and [$^{13}C_5$]–C15iso (**14b**) and [$^{13}C_5$]–C17iso (**15b**) enriched lipids fully rescues ceramide profiles in the *elo-5(gk208)* and *elo-5(gk208); daf-22(ok693)* mutant and confirms that incorporation of L-leucine (**10**) and BCFAs **14b** and **15b** into d17:1iso sphingosine (**17**) depends on the peroxisomal β-oxidation cycle and is strongly attenuated (but not fully abolished) in the *elo-5(gk208); daf-22(ok693)* double mutant (*Table 1*).

Specific incorporation of free isotopically labeled BCFAs (**13b**–**15b**) further revealed *elo-5* independent elongation of C13iso-CoA (**13a**), C15iso-CoA (**14a**), and C17iso-CoA (**15a**) providing a rationale for the incorporation of C13iso (**13b**) into d17:1iso sphingosine (**17**) and its ability to rescue the developmental arrest of *elo-5(gk208; Scheme 2*). However, chain shortening of C17iso-CoA (**15a**) to C15iso-CoA (**14a**) in *elo-5(gk208)* is effectively suppressed in the *elo-5(gk208); daf-22(ok693)* double mutant, providing a molecular basis for the *daf-22* dependency observed for the incorporation of L-leucine (**10**) and BCFA **13b**–**15b** into *C. elegans* ceramides **18**. These results imply that d17:1iso sphingosine (**17**) biosynthesis proceeds through chain elongation to C17iso-CoA (**15a**), which enters the *daf-22* dependent peroxisomal β-oxidation cycle to form the C15iso-CoA building block (**14a**) that condenses with L-serine (**2**) to initiate d17:1iso sphingosine (**17**) biosynthesis (*Scheme 2*). *C. elegans* ceramide biosynthesis in the endoplasmic reticulum thus integrates a catabolic building block derived from the peroxisomal β-oxidation cycle and does not procure the C15iso-CoA unit (**14a**) directly from *de novo* lipogenesis as previously assumed. *Daf-22* dependent chain shortening of C17iso-CoA (**15a**) to C15iso-CoA (**14a**) places the peroxisomal β-oxidation cycle upstream of ceramide **18** biosynthesis and demonstrates that TORC1 dependent nutrient signaling through glucosylceramides **19** also integrates catabolic inputs from the peroxisome.

Most surprisingly, although incorporation of L-leucine (**10**) and BCFAs **13b**–**15b** into the d17:1iso sphingosine moiety (**17**) is strongly suppressed in the *daf-22(ok693)* mutant (*Table 1*), the ceramide **18** profiles of the N2 wildtype and *daf-22(ok693)* lipidome are almost indistinguishable (*Figure 1,c* and *1,d*), suggesting the presence of a L-leucine and BCFA-independent mechanism that compensates the deficiency of *de novo* d17:1iso sphingosine (**17**) biosynthesis in *daf-22(ok693)*. Such an alternative pathway for *de novo* d17:1iso sphingosine (**17**) biosynthesis could in theory recruit an isovalerate (**12**) type building block from isoprenoid metabolism but would also require a parallel pathway for BCFA elongation that circumvents the involvement of the *daf-22*-dependent peroxisomal β-oxidation step that shortens C17iso-CoA (**15a**) by forming the C15iso-CoA (**14a**) building block. Alternatively, it is most conceivable that d17:1iso sphingosine (**17**) recycling within the sphingolipid pool is more pronounced in the *daf-22* mutant (impaired in *de novo* d17:1iso sphingosine biosynthesis) in comparison to the N2 wildtype. In this scenario the metabolic flux through *de novo* d17:1iso sphingosine (**17**) biogenesis and degradation is higher for the N2 wildtype, while the *daf-22* mutant maintains a lower d17:1iso sphingosine (**17**) turnover rate and preserves its ceramide **18** levels by d17:1iso sphingosine (**17**) recycling from the sphingolipid pool. Observation of limited quantities of labeled [$^{13}C_5$]-3-keto sphinganine (**33**) and [$^{13}C_5$]–d17:0iso sphinganine (**34**), along with large quantities of unlabeled *N*-acyl d17:1iso sphingosines (ceramides, **18**) in *daf-22(ok693)*, supports the hypothesis that the unlabeled d17:1iso sphingosine building block (**17**) originates from cleavage of the corresponding sphingomyelins **7** and glucosyl ceramides **8**. The seemingly selective [$^{13}C_5$]-enrichment of very long chain *N*-iso-acyl units in ceramides **18** from the *elo-5; daf-22* double mutant fed with L-[U-$^{13}C_6$]-enriched *B. subtilis ilvB2 leuA169* consequently reflects differences in the metabolic fluxes through the *elo-5* and *daf-22* dependent BCFA elongation pathway for *de novo* d17:1iso sphingosine (**17**) biogenesis versus the *elo-5* and *daf-22* independent *de novo* lipogenesis of C27iso-CoA (**20**), which provides the very long chain *N*-iso-acyl building blocks. Isotope incorporation experiments using synchronized L1 larva to limit the availability of natural abundance sphingolipids might be required to effectively demonstrate the incorporation of L-leucine into d17:1iso sphingosine (**17**) by the *C. elegans daf-22(ok693)* mutant.

However, owing to our current experimental design, our results revealed a largely unrecognized limitation of targeted comparative metabolomics as an established tool in reverse genetics. Changes in metabolic flux through alternative biosynthetic pathways might effectively compensate for the loss of biosynthetic activity in gene deletion mutants, so that metabolite abundances and profiles in wildtype and mutant metabolomes become indistinguishable. In such a scenario, incorporation experiments with isotopically labeled precursors that discriminate between the alternative biosynthetic pathways represent a powerful tool to demonstrate the functional implication of a mutated gene. However, stable isotope incorporation experiments are only rarely performed and commonly require some previous understanding of the gene function in order to design a diagnostic molecular probe. Here, we have synthesized isotopically labeled BCFAs to probe iso-fatty acid metabolism in the *elo-5(gk208)* and *elo-5(gk208); daf-22(ok693* mutants. In order to overcome limitations of precursor uptake and competing metabolism by the bacterial food source, we established the application of isotopically enriched bacterial mutants as a method to examine the incorporation of labeled BCAAs and BCFAs and explore cryptic metabolic pathways in the bacterivorous model organism *C. elegans*.

Experimental Section

Organisms and Culture Conditions

C. elegans wildtype N2 (Bristol), AB1 (Australia), CB4856 (Hawaii), and mutant strains *daf-22(ok693)* RB859, *elo-1(gk48)* VC138, *elo-2(tm12033)*, *elo-3(ok777)* RB910, *elo-3(gk236)* VC545, *elo-4(ok1346)* RB1264, *elo-4(tm1030)*, *elo-5(gk208)* VC410, *elo-5(gk182)* VC377, *elo-6(gk233)* VC425, *elo-8(tm10233)*, *elo-9(ok993)* RB1046, *prx-1(tm392)*, *prx-3(tm6469)*, *prx-5(ku517)* MH5239, *prx-5(tm4948)*, *prx-10(ssd68)* SOZ259, and *elo-5(gk208); daf-22(ok693)* were cultivated at 20 °C on NGM agar seeded with *E. coli* OP50.[59] Axenized *elo-5(gk208)* VC410 and *elo-5(gk208); daf-22(ok693)* were supplemented with BCFA producing *Stenotrophomonas maltophila* or *Bacillus subtilis*, or iso-fatty acids (and their [D_6]-isotopomers) at 0.5 μmol per plate. *C. briggsae* (AF16), *C. brenneri* (PB2801), *C. inopinata* (NKZ35), *C. nigoni* (JU1422), *C. remanei* (PB4641), *C. tropicalis* (JU1373), *C. wallacei* (JU1904), and *Pristionchus pacificus* (RS2333) were grown at 23 °C on NGM agar seeded with *E. coli* OP50.[59] *Panagrellus redivivius* (MT8872) was grown at 23 °C on oatmeal inoculated with *Saccharomyces cerevisiae*. *Turbatrix aceti* was grown at 20 °C on mother of vinegar. *Heterorhabditis*

bacteriophora (EurUS strain) and *Steinernema carpocapsae* (All strain) were cultivated *in vivo* using *Galleria mellonella*. *Escherichia coli* OP50, BL21(DE3), BL21(DE3) *ΔilvD ΔleuB ΔavtA ΔilvE*, and *Bacillus subtilis ilvB2 leuA169* (GB7044) were cultivated at 37 °C in lysogeny broth (LB) medium or M9 minimal medium (5.00 g/L NaCl, 6.00 g/L Na_2HPO_4, 3.00 g/L KH_2PO_4, 1.00 g/L NH_4Cl, 240 mg/L $MgSO_4$ 7 × H_2O, 11.1 mg $CaCl_2$ 2 × H_2O, 3.3 mg/L $FeSO_4$ 7 × H_2O) supplemented with 5.0 g/L D-glucose (or D-[U-$^{13}C_6$]-glucose). Media for BCAA auxotrophs were supplemented with 20 mg/L of L-leucine, L-isoleucine and L-valine, that could be substituted with L-[U-$^{13}C_6$]-leucine or L-[U-$^{13}C_5$]-valine. *C. elegans* wildtype (N2), *daf-22(ok693)*, *elo-5(gk208)*, and *elo-5(gk-208); daf-22(ok693)* were cultivated at 20 °C and 180 rpm in 100 mL S-medium[59] supplemented with natural abundance or isotopically enriched *E. coli* or *B. subtilis* (50 % BCAA enrichment), or *E. coli* supplemented with BCFAs (> 99 % enrichment). After 10 days nematodes were isolated by centrifugation, lyophilized, and their lipidomes extracted and analyzed by HPLC-ESI-HR-MS analysis.

Isolation of Lipids

Nematodes cultivated in S-medium or on NGM plates were washed three times with M9 phosphate buffer at 4 °C and collected by centrifugation at 4500 *g* for 10 min to furnish worm pellets that were frozen at −20 °C and lyophilized. Lipids were extracted using methyl *tert*-butyl methyl ether (MTBE) with vigorous stirring and consecutive sonication for 30 min at 0 °C. After addition of 0.5 mL water the mixture was vortexed and sonicated for 15 min at 0 °C. Phases were separated by centrifugation at 4 °C with 4500 *g* for 15 min. The organic phase was separated and the aqueous phase extracted with 2×1.5 mL MTBE by sonication at 0 °C for 15 min followed by centrifugation at 4 °C with 4500 *g* for 15 min. Lipid extracts were concentrated to dryness under reduced pressure and reconstituted in a mixture of acetonitrile, isopropanol and water (65 : 30 : 5, *v/v/v*) at a concentration of 100 mg dry worms/mL, and analyzed by HPLC-ESI-HR-MS.

HPLC-MS Analysis

Analyses were performed using an Acquity ultra-high-pressure liquid chromatography (UHPLC) system coupled to a Synapt G2 QTOF mass spectrometer (Waters, Milford, MA, USA) controlled by MassLynx 4.1.

Chromatographic separation of lipids was achieved at 80 °C on a Waters Acquity BEH C18 column (100 × 2.1 mm i.d., 1.7 μm particle size) using a binary solvent mixture composed of eluent *A* (water containing 0.1 % formic acid and 10 mM ammonium formate) and eluent *B* (98 % acetonitrile and 2 % water containing 0.1 % formic acid and 10 mM ammonium formate). A linear gradient from 60–100 % *B* in 20 min was applied, followed by a hold at 100 % for 6 min and re-equilibration at 60 % *B* for another 6 min. Analysis was performed using electrospray ionization (ESI) in positive and negative ionization mode using a source temperature of 120 °C, desolvation gas at 15 L/min and 450 °C, capillary voltage at 2.5 kV for ESI-(+) or 2.0 kV for ESI-(−). Mass spectra were recorded from *m/z* 50 to *m/z* 1200. Fragmentation data were collected in data-independent (broad band collision induced dissociation) mode using a collision energy of 8–55 V in positive mode and 10–60 V in negative mode. Data were analyzed with the MassLynx software (Waters, Milford, MA, USA).

Supporting Information

Experimental procedures for the synthesis of BCFAs and supporting figures and tables indicated in the main text.

Acknowledgements

Financial support by the Swiss National Science Foundation (SNSF-169700; SNSF-197228) and the University of Neuchâtel is gratefully acknowledged. Some *C. elegans* mutant strains were generated by the International *C. elegans* Gene Knockout consortium, which is gratefully acknowledged. Some nematode strains were provided by the Caenorhabditis Genetics Center (CGC), which is funded by NIH Office of Research Infrastructure Programs (P40 OD010440). Some nematode strains were provided by the National Bioresource Project (NBRP) for *C. elegans* (Tokyo, Japan). The *B. subtilis* mutant was obtained from the Bacillus Genetic Stock Center (BGSC). We thank Patrick Fallet (University of Neuchatel (UniNE) Switzerland) for EPNs, Chuanfu Dong (Max Planck Institute for Biology, Tübingen, Germany) for *P. pacificus*, and Armelle Vallat (Neuchâtel Platform for Analytical Chemistry (NPAC) Switzerland) for GC-EIMS measurements. Open Access funding provided by Universite de Neuchatel.

Data Availability Statement

The data that support the findings of this study are available from the corresponding author upon reasonable request.

Author Contribution Statement

R. R. S., *S. B.*, *M.-D. S.*, performed experiments, *R. R. S.* and *H. L.* performed total synthesis, *S. H. v. R.* and *R. R. S.* analyzed the data and wrote the article with contributions from all authors. *B. W. F.* and *Y. I.* contributed reagents. *S. S.* and *G. G.* acquired MS data. *S. H. v. R.* conceived and designed the experiments.

References

[1] A. H. Merrill Jr., 'Sphingolipid and Glycosphingolipid Metabolic Pathways in the Era of Sphingolipidomics', *Chem. Rev.* **2011**, *111*, 6387–6422.

[2] S. Lahiri, A. H, Futerman, 'The metabolism and function of sphingolipids and glycosphingolipids', *Cell. Mol. Life Sci.* **2007**, *64*, 2270–2284.

[3] B. M. Quinville, N. M. Deschenes, A. E. Ryckman, J. S. Walia, 'A Comprehensive Review: Sphingolipid Metabolism and Implications of Disruption in Sphingolipid Homeostasis', *Int. J. Mol. Sci.* **2021**, *22*, 5793.

[4] Y. A. Hannun, L. M. Obeid, 'Sphingolipids and their metabolism in physiology and disease', *Nat. Rev. Mol. Cell Biol.* **2018**, *19*, 175–191.

[5] G. Tettamanti, R. Bassi, P. Viani, L. Riboni, 'Salvage pathways in glycosphingolipid metabolism', *Biochimie* **2003**, *85*, 423–437.

[6] K. Kitatani, J. Idkowiak-Baldys, Y. A. Hannun, 'The sphingolipid salvage pathway in ceramide metabolism and signaling', *Cell. Signalling* **2008**, *20*, 1010–1018.

[7] T. Wakashima, K. Abe, A. Kihara, 'Dual Functions of the *Trans*-2-Enoyl-CoA Reductase TER in the Sphingosine 1-Phosphate Metabolic Pathway and in Fatty Acid Elongation', *J. Biol. Chem.* **2014**, *289*, 24736–24748.

[8] A. Kihara, 'Sphingosine 1-phosphate is a key metabolite linking sphingolipids to glycerophospholipids', *Biochim. Biophys. Acta* **2014**, *1841*, 766–772.

[9] W.-J. Park, J.-W. Park, 'The effect of altered sphingolipid acyl chain length on various disease models', *Biol. Chem.* **2015**, *396*, 693–705.

[10] M.-S. Wegner, S. Schiffmann, M. J. Parnham, G. Geisslinger, S. Grösch, 'The enigma of ceramide synthase regulation in mammalian cells', *Prog. Lipid Res.* **2016**, *63*, 93–119.

[11] S. T. Pruett, A. Bushnev, K. Hagedorn, M. Adiga, C. A. Haynes, M. C. Sullards, D. C. Liotta, A. H. Merrill Jr, 'Biodiversity of sphingoid bases ("sphingosines") and related amino alcohols', *J. Lipid Res.* **2008**, *49*, 1621–1639.

[12] M. Witting, P. Schmitt-Kopplin, 'The *Caenorhabditis elegans* lipidome: A primer for lipid analysis in *Caenorhabditis elegans*', *Arch. Biochem. Biophys.* **2016**, *589*, 27–37.

[13] B. Spanier, A. Laurençon, A. Weiser, N. Pujol, S. Omi, A. Barsch, A. Korf, S. W. Meyer, J. J. Ewbank, F. Paladino, S. Garvis, H. Aguilaniu, M. Witting, 'Comparison of lipidome profiles of *Caenorhabditis elegans*-results from an inter-laboratory ring trial', *Metabolomics* **2021**, *17*, 25.

[14] L. An, X. Fu, J. Chen, J. Ma, 'Application of *Caenorhabditis elegans* in Lipid Metabolism Research', *Int. J. Mol. Sci.* **2023**, *24*, 1173.

[15] X. Deng, R. Kolesnick, '*Caenorhabditis elegans* as a model to study sphingolipid signaling', *Biol. Chem.* **2015**, *396*, 767–773.

[16] V. Hänel, C. Pendleton, M. Witting, 'The sphingolipidome of the model organism *Caenorhabditis elegans*', *Chem. Phys. Lipids* **2019**, *222*, 15–22.

[17] X. Cheng, X. Jiang, K. Y. Tam, G. Li, J. Zheng, H. Zhang, 'Sphingolipidomic Analysis of *C. elegans* reveals Development- and Environment-dependent Metabolic Features', *Int. J. Biol. Sci.* **2019**, *15*, 2897–2910.

[18] J. Scholz, P. O. Helmer, M. M. Nicolai, J. Bornhorst, H. Hayen, 'Profiling of sphingolipids in *Caenorhabditis elegans* by two-dimensional multiple heart-cut liquid chromatography – mass spectrometry', *J. Chromatogr. A.* **2021**, *1655*, 462481.

[19] D. J. Chitwood, W. R. Lusby, M. J. Thompson, J. P. Kochansky, O. W. Howarth, 'The glycosylceramides of the nematode *Caenorhabditis elegans* contain an unusual, branched-chain sphingoid base', *Lipids* **1995**, *30*, 567–573.

[20] S. Gerdt, G. Lochnit, R. D. Dennis, R. Geyer, 'Isolation and structural analysis of three neutral glycosphingolipids from a mixed population of *Caenorhabditis elegans* (Nematoda: Rhabditida)', *Glycobiology* **1997**, *7*, 265–275.

[21] S. Gerdt, R. D. Dennis, G. Borgonie, R. Schnabel, R. Geyer, 'Isolation, characterization and immunolocalization of phosphorylcholine-substituted glycolipids in developmental stages of *Caenorhabditis elegans*', *Eur. J. Biochem.* **1999**, *266*, 952–963.

[22] G. Lochnit, R. D. Dennis, U. Zähringer, R. Geyer, 'Structural analysis of neutral glycosphingolipids from *Ascaris suum* adults (Nematoda: Ascaridida)', *Glycoconjugate J.* **1997**, *14*, 389–399.

[23] G. Lochnit, S. Nispel, R. D. Dennis, R. Geyer, 'Structural analysis and immunohistochemical localization of two acidic glycosphingolipids from the porcine, parasitic nematode, *Ascaris suum*', *Glycobiology* **1998**, *8*, 891–899.

[24] H. Zhu, H. Shen, A. K. Sewell, M. Kniazeva, M. Han, 'A novel sphingolipid-TORC1 pathway critically promotes postembryonic development in *Caenorhabditis elegans*', *eLife* **2013**, *2*, e00429.

[25] N. Li, B. Hua, Q. Chen, F. Teng, M. Ruan, M. Zhu, L. Zhang, Y. Huo, H. Liu, M. Zhuang, H. Shen, H. Zhu, 'A sphingolipid-mTORC1 nutrient-sensing pathway regulates animal development by an intestinal peroxisome relocation-based gut-brain crosstalk', *Cell Rep.* **2022**, *40*, 111140.

[26] M. Kniazeva, H. Zhu, A. K. Sewell, M. A. Han, 'A Lipid-TORC1 Pathway Promotes Neuronal Development and Foraging Behavior under Both Fed and Fasted Conditions in *C. elegans*', *Dev. Cell.* **2015**, *33*, 260–271.

[27] R. G. Cutler, K. W. Thompson, S. Camandola, K. T. Mack, M. P. Mattson, 'Sphingolipid metabolism regulates development and lifespan in *Caenorhabditis elegans*', *Mech. Ageing Dev.* **2014**, *143–144*, 9–18.

[28] F. Wang, Y. Dai, X. Zhu, Q. Chen, H. Zhu, B. Zhou, H. Tang, S. Pang, 'Saturated very long chain fatty acid configures glycosphingolipid for lysosome homeostasis in long-lived *C. elegans*', *Nat. Commun.* **2021**, *12*, 5073.

[29] M. Cui, Y. Wang, J. Cavaleri, T. Kelson, Y. Teng, M. Han, 'Starvation-Induced Stress Response Is Critically Impacted by Ceramide Levels in *Caenorhabditis elegans*', *Genetics* **2017**, *205*, 775–785.

[30] M. A. Xatse, A. F. C. Vieira, C. Byrne, C. P. Olsen, 'Targeted lipidomics reveals a novel role for glucosylceramides in glucose response', *J. Lipid Res.* **2023**, *64*, 100394.

[31] H. Zhu, A. K. Sewell, M. Han, 'Intestinal apical polarity mediates regulation of TORC1 by glucosylceramide in *C. elegans*', *Genes Dev.* **2015**, *29*, 1218–1223.

[32] K. H. Nomura, D. Murata, Y. Hayashi, K. Dejima, S. Mizuguchi, E. Kage-Nakadai, K. Gengyo-Ando, S. Mitani, Y. Hirabayashi, M. Ito, K. Nomura, 'Ceramide glucosyltransferase of the nematode *Caenorhabditis elegans* is involved in oocyte formation and in early embryonic cell division', *Glycobiology* **2011**, *21*, 834–848.

[33] T. K. Blackwell, A. K. Sewell, Z. Wu, M. Han, 'TOR Signaling in *Caenorhabditis elegans* Development, Metabolism, and Aging', *Genetics* **2019**, *213*, 329–360.

[34] M. Kniazeva, Q. T. Crawford, M. Seiber, C.-Y. Wang, M. Han, 'Monomethyl Branched-Chain Fatty Acids Play an Essential Role in *Caenorhabditis elegans* Development', *PLoS Biol.* **2004**, *2*, e257.

[35] M. Kniazeva, T. Euler, M. Han, 'A branched-chain fatty acid is involved in post-embryonic growth control in parallel to the insulin receptor pathway and its biosynthesis is feedback-regulated in *C. elegans*', *Genes* **2008**, *22*, 2102–2110.

[36] M. Kniazeva, H. Shen, T. Euler, C. Wang, M. Han, 'Regulation of maternal phospholipid composition and IP_3-dependent embryonic membrane dynamics by a specific fatty acid metabolic event in *C. elegans*', *Genes Dev.* **2012**, *26*, 554–566.

[37] J. Zhang, Y. Hu, Y. Wang, L. Fu, X. Xu, C. Li, J. Xu, C. Li, L. Zhang, R. Yang, X. Jiang, Y. Wu, P. Liu, Y. Zou, B. Liang, 'mmBCFA C17iso ensures endoplasmic reticulum integrity for lipid droplet growth', *J. Cell Biol.* **2021**, *220*, e202102122.

[38] J. T. Hannich, D. Mellal, S. Feng, A. Zumbuehl, H. Riezman, 'Structure and conserved function of iso-branched sphingoid bases from the nematode *Caenorhabditis elegans*', *Chem. Sci.* **2017**, *8*, 3676–3686.

[39] C. L. Perez, M. R. Van Gilst, 'A ^{13}C Isotope Labeling Strategy Reveals the Influence of Insulin Signaling on Lipogenesis in *C. elegans*', *Cell Metab.* **2008**, *8*, 266–274.

[40] E. V. Entchev, D. Schwudke, V. Zagoriy, V. Matyash, A. Bogdanova, B. Habermann, L. Zhu, A. Shevchenko, T. V. Kurzchalia, 'LET-767 Is Required for the Production of Branched Chain and Long Chain Fatty Acids in *Caenorhabditis elegans*', *J. Biol. Chem.* **2008**, *283*, 17550–17560.

[41] F. Jia, M. Cui, M. T. Than, M. Han, 'Developmental Defects of *Caenorhabditis elegans* Lacking Branched-chain α-Ketoacid Dehydrogenase Are Mainly Caused by Monomethyl Branched-chain Fatty Acid Deficiency', *J. Biol. Chem.* **2016**, *291*, 2967–2973.

[42] S. Zdraljevic, B. W. Fox, C. Strand, O. Panda, F. J. Tenjo, S. C. Brady, T. A. Crombie, J. G. Doench, F. C. Schroeder, E. C. Andersen, 'Natural variation in *C. elegans* arsenic toxicity is explained by differences in branched chain amino acid metabolism', *eLife* **2019**, *8*, e40260.

[43] M. Zhu, F. Teng, N. Li, L. Zhang, S. Zhang, F. Xu, J. Shao, H. Sun, H. Zhu, 'Monomethyl branched-chain fatty acid mediates amino acid sensing upstream of mTORC1', *Dev. Cell.* **2021**, *56*, 2692–2702.e5.

[44] E. Seamen, J. M. Blanchette, M. Han, 'P-type ATPase TAT-2 Negatively Regulates Monomethyl Branched-Chain Fatty Acid Mediated Function in Post-Embryonic Growth and Development in *C. elegans*', *PLoS Genet.* **2009**, *5*, e1000589.

[45] R. Wang, M. Kniazeva, M. Han, 'Peroxisome Protein Transportation Affects Metabolism of Branched-Chain Fatty Acids That Critically Impact Growth and Development of *C. elegans*', *PLoS One* **2013**, *8*, e76270.

[46] S. H. von Reuss, N. Bose, J. Srinivasan, J. J. Yim, J. C. Judkins, P. W. Sternberg, F. C. Schroeder, 'Comparative Metabolomics Reveals Biogenesis of Ascarosides, a Modular Library of Small-Molecule Signals in *C. elegans*', *J. Am. Chem. Soc.* **2012**, *134*, 1817–1824.

[47] E. Marza, K. T. Simonsen, N. J. Færgeman, G. M. Lesa, 'Expression of ceramide glucosyltransferases, which are essential for glycosphingolipid synthesis, is only required in a small subset of *C. elegans* cells', *J. Cell Sci.* **2009**, *122*, 822–833.

[48] D. Park, I. O'Doherty, R. K. Somvanshi, A. Bethke, F. C. Schroeder, U. Kumar, D. L. Riddle, 'Interaction of structure-specific and promiscuous G-protein–coupled receptors mediates small-molecule signaling in *Caenorhabditis elegans*', *Proc. Natl. Acad. Sci. USA* **2012**, *109*, 9917–9922.

[49] M. Gu, J. L. Kerwin, J. D. Watts, R. Aebersold, 'Ceramide Profiling of Complex Lipid Mixtures by Electrospray Ionization Mass Spectrometry', *Anal. Biochem.* **1997**, *244*, 347–356.

[50] N. Kanzaki, I. J. Tsai, R. Tanaka, V. L. Hunt, D. Liu, K. Tsuyama, Y. Maeda, S. Namai, R. Kumagai, A. Tracey, N. Holroyd, S. R. Doyle, G. C. Woodruff, K. Murase, H. Kitazume, C. Chai, A. Akagi, O. Panda, H.-M. Ke, F. C. Schroeder, J. Wang, M. Berriman, P. W. Sternberg, A. Sugimoto, T. Kikuchi, 'Biology and genome of a newly discovered sibling species of *Caenorhabditis elegans*', *Nat. Commun.* **2018**, *9*, 3216.

[51] M.-A. Félix, C. Braendle, A. D. Cutter, 'A Streamlined System for Species Diagnosis in *Caenorhabditis* (Nematoda: Rhabditidae) with Name Designations for 15 Distinct Biological Species', *PLoS One* **2014**, *9*, e94723.

[52] Z. Wang, D. H. Wang, H. G. Park, Y. Yan, Y. Goykhman, P. Lawrence, K. S. D. Kothapalli, J. T. Brenna, 'Identification of genes mediating branched chain fatty acid elongation', *FEBS Lett.* **2019**, *593*, 1807–1817.

[53] M. B. Richardson, S. J. Williams, 'A practical synthesis of long-chain iso-fatty acids (iso-C_{12}–C_{19}) and related natural products', *Beilstein J. Org. Chem.* **2013**, *9*, 1807–1812.

[54] J. D. Nickels, S. Chatterjee, B. Mostofian, C. B. Stanley, M. Ohl, P. Zolnierczuk, R. Schulz, D. A. A. Myles, R. F. Standaert, J. G. Elkins, X. Cheng, J. Katsaras, '*Bacillus subtilis* Lipid Extract, A Branched-Chain Fatty Acid Model Membrane', *J. Phys. Chem. Lett.* **2017**, *8*, 4214–4217.

[55] V. Menuz, K. S. Howell, S. Gentina, S. Epstein, I. Riezman, M. Fornallaz-Mulhauser, M. O. Hengartner, M. Gomez, H. Riezman, J. C. Martinou, 'Protection of *C. elegans* from anoxia by HYL-2 ceramide synthase', *Science* **2009**, *324*, 381–384.

[56] M.-B. Mosbech, R. Kruse, E. B. Harvald, A. S. Braun Olsen, S. Fernandez Gallego, H. K. Hannibal-Bach, C. S. Ejsing, N. J. Færgeman, 'Functional Loss of Two Ceramide Synthases Elicits Autophagy-Dependent Lifespan Extension in *C. elegans*', *PLoS One* **2013**, *8*, e70087.
[57] T. A. Staab, G. McIntyre, L. Wang, J. Radeny, L. Bettcher, M. Guillen, M. P. Peck, A. P. Kalil, S. P. Bromley, D. Raftery, J. P. Chan, 'The lipidomes of *C. elegans* with mutations in *asm-3*/acid sphingomyelinase and *hyl-2*/ceramide synthase show distinct lipid profiles during aging', *Aging* **2023**, *15*, 650–674.
[58] Y. Li, C. Wang, Y. Huang, R. Fu, H. Zheng, Y. Zhu, X. Shi, P. K. Padakanti, Z. Tu, X. Su, H. Zhang, '*C. Elegans* Fatty Acid Two-Hydroxylase Regulates Intestinal Homeostasis by Affecting Heptadecenoic Acid Production', *Cell. Physiol. Biochem.* **2018**, *49*, 947–960.
[59] T. Stiernagle, 'Maintenance of *C. elegans*', in 'WormBook', Ed. The *C. elegans* Research Community, WormBook, 2006, http://www.wormbook.org/chapters/www_strainmaintain/strainmaintain.html.

Received July 31, 2023
Accepted September 28, 2023

